AGU PUBLICATIONS

JGR

Journal of Geophysical Research: Oceans

RESEARCH ARTICLE

10.1002/2014JC009809

Key Points:
- Chlorophyll-rich water is conveyed to the Gulf Stream within a shelf-edge jet
- The zone of shelf water export to the Gulf Stream rapidly shifts in latitude
- The shifts are linked to movement of the Gulf Stream/margin separation

Correspondence to:
J. H. Churchill,
jchurchill@whoi.edu

Citation:
Churchill, J. H., and G. G. Gawarkiewicz (2014), Shelf water and chlorophyll export from the Hatteras slope and outer shelf, *J. Geophys. Res. Oceans*, *119*, 4291–4304, doi:10.1002/2014JC009809.

Received 10 JAN 2014
Accepted 28 MAY 2014
Accepted article online 3 JUN 2012
Published online 16 JULY 2014

Shelf water and chlorophyll export from the Hatteras slope and outer shelf

James H. Churchill[1] and Glen G. Gawarkiewicz[1]

[1]Physical Oceanography Department, Woods Hole Oceanographic Institution, Woods Hole, Massachusetts, USA

Abstract Using high-resolution data acquired from a shipboard ADCP and a towed Scanfish equipped with a CTD and fluorometer, we examine the properties and transport of Middle Atlantic Bight (MAB) shelf water over a region of the Hatteras outer shelf and slope where MAB shelf water is commonly deflected offshore and entrained into the Gulf Stream. The data are from a period in early August 2004 when the seasonal pycnocline of the MAB is well developed and situated over a weakly stratified, near-bottom shelf water mass commonly referred to as the cold pool. Our data show chlorophyll-rich cold pool water carried rapidly southward over the slope and outer shelf, at a rate of up to 60 cm s^{-1}, as part of the shelf-edge frontal jet. This southward transport of chlorophyll-rich cold pool water is shunted eastward and entrained into the Gulf Stream. However, the latitude band over which this export occurs varies significantly over the 7 day course of our study, a variation which is linked to an order 50 km shift in the latitude at which the Gulf Stream separates from the continental margin. The coupled rapid translation of the Gulf Stream frontal separation and the cold pool export zone is likely to have a significant impact on the movement and accumulation of biogenic material over the Hatteras slope and rise.

1. Introduction

The oceanic region near Cape Hatteras, NC marks the terminus of the southward-trending flow of Middle Atlantic Bight (MAB) shelf water (salinity < 34 psu), which is a part of a longer equatorward coastal current originating on the Greenland/Labrador shelf [*Chapman and Beardsley*, 1989]. The sum of numerous observations indicates that the preponderance of MAB shelf water flow shunted offshore near Cape Hatteras is entrained into the Gulf Stream, which separates from the continental margin in the vicinity of Cape Hatteras [*Ford et al*., 1952; *Fisher*, 1972; *Kupferman and Garfield*, 1977; *Churchill et al*., 1989; *Lillibridge et al*., 1990; *Wood et al*., 1996; *Churchill and Berger*, 1998; *Gawarkiewicz and Linder*, 2006; *Gawarkiewicz et al*., 2008; *Churchill and Gawarkiewicz*, 2012]. Coupled with the offshore shelf water flow near Cape Hatteras is a substantial seaward export of organic matter produced over the MAB shelf and upper slope. This export is indicated by a relatively large accumulation rate of organic carbon over the slope east of Cape Hatteras (order 10 moles C m^{-2} yr^{-1} as compared with order 2 moles C m^{-2} yr^{-1} over the MAB slope to the north) [*Alperin et al*., 2002; *DeMaster et al*., 1994, 2002; *Thomas et al*., 2002]. Further evidence of organic carbon export near Cape Hatteras comes from analysis of CTD and fluorescence measurements by *Wood et al*. [1996], which reveals transfer of chlorophyll-rich MAB shelf water from beneath the seasonal pycnocline to the edge of the Gulf Stream.

Recently, *Churchill and Gawarkiewicz* [2012] examined patterns of MAB shelf water flow and export near Cape Hatteras using CTD and velocity data from the mooring array of the Ocean Margins Program [*Verity et al*., 2002]. Their analysis revealed two primary transport pathways by which MAB shelf water entering the Hatteras region is conveyed offshore [see *Churchill and Gawarkiewicz*, 2012, Figure 12]. Water entering the Hatteras region over the middle and inner shelf (bottom depths < 40 m) tends to experience very little loss over the latitude range of the OMP array (35°27′N–36°40′N). Churchill and Gawarkiewicz hypothesized that this water is likely diverted offshore upon encountering the Hatteras Front, which separates MAB shelf water from the more saline shelf water of the South Atlantic Bight [*Churchill and Berger*, 1998; *Savidge and Austin*, 2007; *Savidge et al*., 2013a, 2013b]. By contrast, MAB shelf water flow seaward of the shelf edge is exported over the length of the mooring array, essentially vanishing by the southern extreme of the array. Notably, this flow encompasses much of the shelf-edge frontal jet, which typically extends beyond the shelf edge and contains a transport of order 0.25 Sv with maximum velocities of order 0.3 m s^{-1} [*Linder and Gawarkiewicz*, 1998; *Fratantoni et al*., 2001; *Gawarkiewicz and Linder*, 2006].

A number of questions remain regarding the export of MAB shelf water in the Hatteras region. With regard to shelf water export from the slope, it is unclear to what extent biogenic material is contained in the shelf-edge frontal jet and transported offshore (i.e., is there a large export of organic carbon associated with entrainment of the frontal jet into the Gulf Stream?). It is also unclear how movements of the Gulf Stream front may influence the flow of shelf water over the slope or the latitude at which it is deflected offshore.

We address these and related issues using CTD/fluorescence/velocity data acquired from a towed vehicle and a shipboard ADCP in the shelf-edge frontal jet export zone identified by *Churchill and Gawarkiewicz* [2012].

2. Methods

The data used in our study were acquired as part of the August 2004 field operations of the Frontal Interaction Near Cape Hatteras (FINCH) program. These operations involved deployment and recovery of instrumented moorings, as well as simultaneous data collection from two research vessels: the *R/V Slover* operating near Cape Hatteras in the area of the Hatteras Front [*Savidge and Austin*, 2007] and the *R/V Cape Henlopen* operating principally over the slope and outer shelf further north. Our study focused on data acquired from the *Cape Henlopen* in the 35°35′N to 36°20′N latitude band, and from a pair of moorings deployed over the upper slope (at ∼80 m depth) near 35°45′N (Figure 1).

The *Cape Henlopen* operations began on 4 August with the deployment of the mooring pair. One mooring consisted of a tripod outfitted with an upward-looking, 300 kHz Acoustic Doppler Current Profiler (ADCP). The second was comprised of a string of 12 thermistors (Onset Computer Corp. Tidbit temperature loggers) distributed, from <1 m below the surface to ∼5 m above bottom, on a line supported by a surface float. Single-ping measurements from the ADCP, acquired at a rate of 1.8 s per ping, were averaged over 15 min intervals to give vertical profiles of horizontal velocity in 1 m depth bins from roughly 6 m below the surface to 4 m above the bottom. The thermistors were programmed to give temperature measurements at 15 min intervals.

Following the mooring deployment, water properties over the outer shelf and slope were surveyed using a Geological and Marine Instrumentation model MKII "Scanfish" towed from the *Cape Henlopen*. The Scanfish was outfitted with a Sea-Bird model 911+ CTD, a WET Labs WS3S fluorometer and a Sea-Bird SBE 43 oxygen sensor. Data were acquired from these instruments with ship steaming at roughly six knots and the Scanfish undulating roughly between 2 and 120 m depth (or to within a few meters of the bottom in water shallower than 120 m). Horizontal spacing between the shallowest points of an undulation cycle ranged from 500 m in shallow water to 2 km in deep water. The measurements from each full undulation (ascending and descending) cycle were averaged into a single vertical profile.

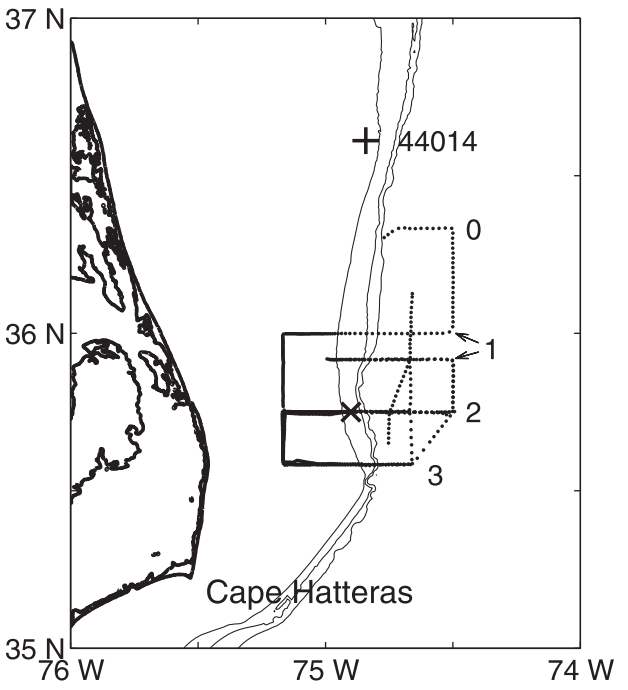

Figure 1. The Hatteras shelf and slope. The dots mark the centers of Scanfish profiles used in our study, with east-west transects identified. The "cross" marks the location of the ADCP/thermistor-string mooring and the "plus" is the site of NOAA meteorological buoy 44014. The gray lines mark the 60, 100, and 200 m isobaths.

Throughout the cruise, velocity profiles were acquired from the *Cape Henlopen*'s 600 kHz hull-mounted ADCP. The ADCP data were averaged over 5 min intervals to give profiles of horizontal velocity in 1 m depth bins.

Barotropic tidal currents were removed from these profiles using results of tidal simulations computed by the finite element model ADCIRC [*Luettich et al*., 1992] over a North Atlantic model grid [see *Blanton et al*., 2004]. Computed tidal currents over the Scanfish tracks were no larger than 0.08 m s^{-1} and were $<$0.03 m s^{-1} at bottom depths $>$100 m. Unfortunately, due to the high acoustic frequency of the *Cape Henlopen*'s ADCP, its measurement depth range was limited to $\sim$5–40 m.

Scanfish surveying was carried out over 5–11 August, after which the mooring pair was recovered. Surveying was done over transects oriented across and along the shelf/slope and with the ship trending either northward or southward while covering the transects. We have divided the survey into five phases, each of which consists of a single transit over the survey region (35°35′N–36°20′N). Here particular attention is given to the measurements from the four east-west transects (Figure 1), designated as transect: 0—along 36°20′ (covered in phase 1 only); 1—36°00′ (phase 1) or 35°55′ (phases 3–5); 2—35°45′; and 3—35°35′.

The wind velocity data used in our study were from NOAA buoy 44014 (Figure 1) and were supplied by the National Data Buoy Center (http://www.ndbc.noaa.gov/). Satellite radiometer-derived images of sea surface temperature (SST) were obtained from the Rutgers University Coastal Ocean Observation Laboratory SST image archive.

A focus of our study was on the distribution and transport of organic material in the region of the Hatteras slope and outer shelf. However, we acquired no data from this region to relate the Scanfish fluorometer voltage to chlorophyll concentration, and thus could not confidently convert the fluorometer's measurements to chlorophyll concentrations. As a proxy for chlorophyll concentration, we used the quantity $F_V = V - V_{min}$, where V is the fluorometer output voltage and V_{min} is the fluorometer's lowest output voltage (0.056 V), which is presumably roughly equal to the instrument's clear water voltage. Previous investigators of the chlorophyll distribution in our study region [*Wood et al*., 1996; *Lohrenz et al*., 2002] have reported a strong statistical relationship between chlorophyll concentration determined from analysis of water samples and the fluorescence signal of a fluorometer attached to a shipboard CTD. In particular, *Wood et al*. [1996] found a linear relationship with $R^2 = 0.906$ between the chlorophyll concentrations of water samples taken between 35.3°N and 36.4°N over the Hatteras shelf and slope (from a bottom depth range of 28–600 m) and in situ fluorescence measured at the water sample locations and times.

In assuming a proportional relationship between fluorometer voltage and chlorophyll concentration, the possible impact of colored dissolved organic matter (CDOM) on fluorescence measurements must be considered. *Vodacek et al*. [1997] examined fluorescence measurements acquired from a CDOM-sensitive fluorometer, with 355 nm excitation and 450 nm emission wavelengths, over a track extending from mouth of Delaware Bay southeast to the Sargasso Sea. They reported measurable CDOM fluorescence over the full track line. The fluorometer used in our study was designed as a chlorophyll-sensitive device, with 460 and 695 nm excitation and emission frequencies, respectively. To estimate the impact of CDOM on the voltage measurements of this fluorometer, we converted CDOM measurements acquired from an autonomous biogeochemical float [*Barnard and Mitchell*, 2013] (http://navis.sea-birdscientific.com/profilemap.php?floatId=32) over the shelf edge and slope north of our study region to fluorometer voltage using the relationship derived by *Proctor and Roesler* [2010] for a 470 nm excitation wavelength (their Figure 4b). The results indicate an order 10–30 mV response by our fluorometer to the CDOM concentrations expected in our study region. As reported below, the F_V values used in our analysis span a 1 V range, which we may assume is principally the result of chlorophyll fluorescence.

3. Results

3.1. Water Mass Properties

The temperature/salinity (T/S) properties of the water sampled by the Scanfish show a number of distinct water masses as well as mixtures of these masses (Figure 2). In the salinity band of MAB shelf water, weakly stratified and relatively cold subsurface water, commonly referred to as cold pool water, is evident. Typically residing over the middle and outer shelf of the MAB, cold pool water is as a remnant of water formed in the winter that has been capped by the seasonal pycnocline [*Bigelow*, 1933; *Han and Niedrauer*, 1981; *Houghton et al*., 1982; *Flagg et al*., 1998; *Bignami and Hopkins*, 2003]. It is situated shoreward of the shelf-edge front and is generally bordered inshore by coastal water that is warmer due to vertical mixing induced by the tides and wind. The cold pool water observed in our survey has a vertical density stratification of order 1 σ_T

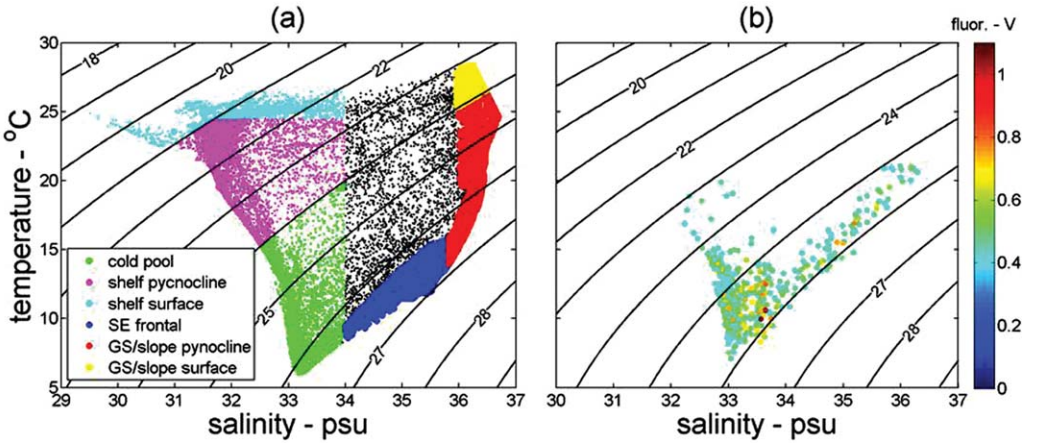

Figure 2. (a) Temperature/salinity (T/S) characteristics of all Scanfish measurements at the locations shown in Figure 1. The water mass identifications are based on examination of vertical T, S, and velocity profiles derived from the Scanfish and ADCP data and T, S data taken as part of other studies conducted in the MAB. Abbreviations are SE, shelf edge and GS, Gulf Stream. (b) T/S characteristics and F_V of only those samples with $F_V > 0.4$ V.

over 25 m and an upper σ_T bound of ~26.4. Its lower σ_T bound varies between 24 and 24.5. Hereafter, the σ_T range of cold pool water is specified as 24–26.4. In our survey data, the cold pool water is situated beneath a pycnocline (with density varying by order 3 σ_T over 5 m), which in turn is beneath a weakly stratified 5–20 m deep surface layer with T > 23°C.

Other water masses captured by the survey, and identified by their T/S properties, include: surface and upper pycnocline Gulf Stream water, MAB slope water, MAB shelf/slope frontal water and frontal water separating near-surface Gulf Stream and MAB shelf waters (Figure 2).

Values of fluorometer voltage (F_V) indicate that the highest chlorophyll concentrations are in water of 24–26.2 σ_T (Figure 2). Furthermore, the highest F_V are predominately from the cold pool. Of those F_V in excess of 0.4 V, 83% are from cold pool samples (i.e., $24 < \sigma_T < 26.4$; S < 34).

The vertical distribution of F_V, represented here by averages over 5 m depth bins (Figure 3), indicates that much of the chlorophyll sampled by our survey is from the 20 to 60 m depth band. The highest 5 m F_V averages are within the 20–40 m depth band. With regard to the computation of the F_V fluxes (a proxy for chlorophyll flux) to be presented later, the preponderance of high F_V in this depth band is fortuitous as is overlaps the limited depth range (~5–40 m) of the ADCP velocity measurements.

3.2. Gulf Stream Frontal Movement

During the 7 days of our survey, the Gulf Stream frontal configuration seaward of the Hatteras shelf changed significantly, as evidenced by the SST imagery of the period (Figure 4).

SST imagery from the first survey phase (5–6 August) shows the Gulf Stream separating from the continental margin at roughly 35°38′ N. To the east of this separation point, a band of cold water is seen extending along the northern margin of the Stream. This is presumably the signature of MAB shelf water entrained into the Gulf Stream and carried eastward.

Imagery of the second survey phase (6–7 August) is more challenging to interpret. Two surface temperature fronts appear east of the Hatteras shelf. One is near the shelf edge and separates 24 and 27°C surface waters (the latter represented as a yellow area in Figure 4). The second front is further east and separates 27 and 28.5°C surface waters (represented by yellow and orange, respectively, in Figure 4). Based on the sequence of SST images from this period (four clear images over 7–8 August), and the ADCP data acquired over the slope in the area of the first front described above (which show southward flow of the warm water seaward of this front), we hypothesize the ~27°C water appearing between the fronts is the surface expression of water that had been expelled from the Gulf Stream after it separated from the continental margin. Such parcels of expelled Gulf Stream water have been described by *Churchill and Cornillon* [1991a, 1991b]. The observations of *Churchill and Cornillon* [1991a] indicate that such parcels are comprised of Gulf Stream

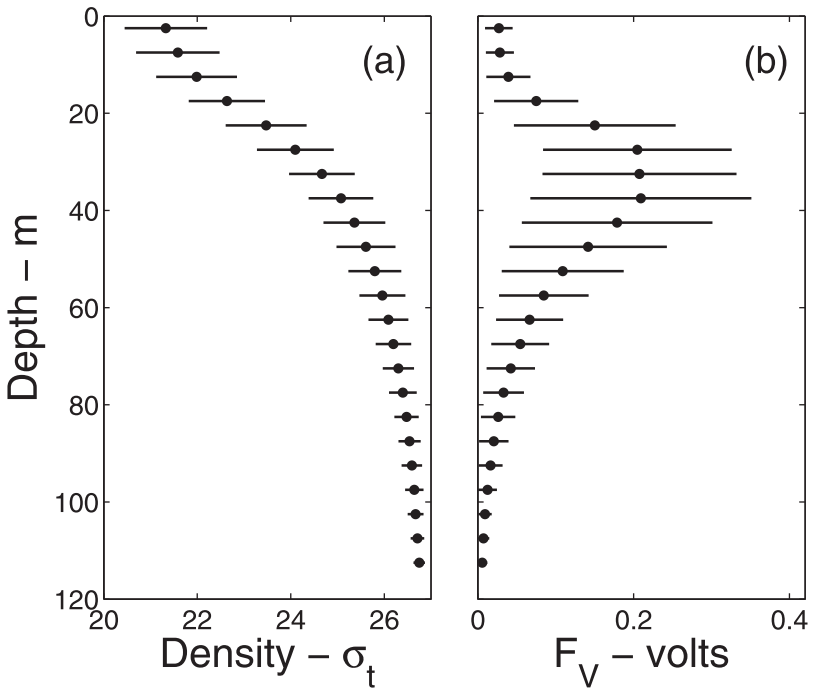

Figure 3. Averages of (a) σ_T and (b) F_V, together with standard deviations about the averages, from Scanfish profiles acquired at the locations shown in Figure 1.

water which had upwelled along isopycnals before being expelled from the Stream, and that they contain relatively weak velocities compared with surface Gulf Stream flow.

The edge of the Gulf Stream, and its separation from the continental margin, is clearly defined in the imagery of survey phase 3 (Figure 4). A band of cold water, presumably entrained MAB shelf water, is seen along the northern margin of the Gulf Stream downstream of its separation point. What may be a remnant of the 27°C surface water seen in the phase 2 imagery (and identified as expelled Gulf Stream water) appears to the north of this cold water band.

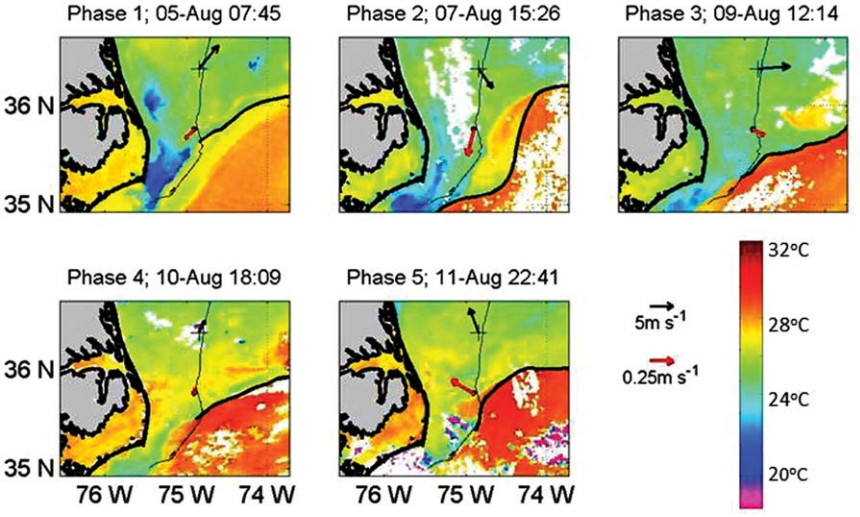

Figure 4. Satellite AVHRR-derived images of SST of each survey phase. The red vectors show near-surface (7 m) velocity at the time of the image taken from the low-pass filtered (10 h half-power point) velocity record of the moored ADCP. Black vectors are wind velocity at the time of the image taken from the buoy 44014 wind record (to constrain the image borders, the vector origin is 0.25° south of the 44014 location). The narrow black line marks the 100 m isobath. Thick black lines trace the Gulf Stream edge. Image times are in GMT.

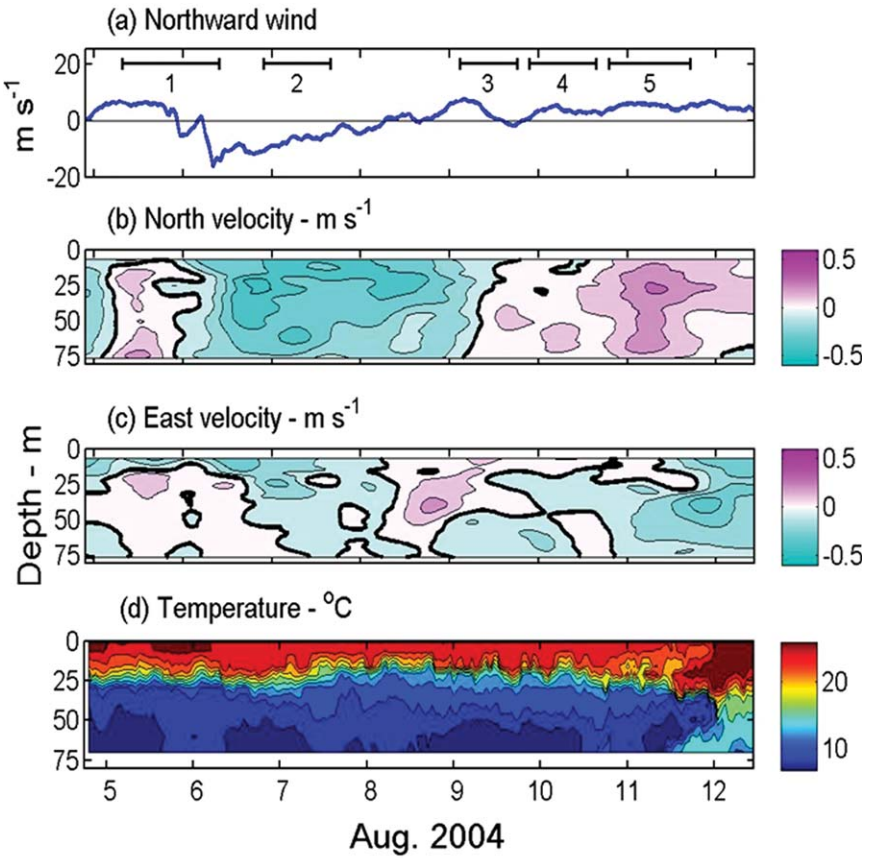

Figure 5. Time series of temperature and velocity measured at the upper slope mooring, as well as northward wind velocity measured at NOAA buoy 44014 (Figure 1). The water velocity time series have been low-pass filtered with a 10 h half-power point filter. Times of the survey phases are shown in Figure 5a.

The Gulf Stream's edge and the location at which is separates from the continental margin are also well defined in the SST imagery of survey phases 4 and 5 (Figure 4). The imagery of phase 5 shows a band of warm water, centered at roughly 35°35′N, extending from the Gulf Stream edge onto the shelf, presumably the signature of a shoreward intrusion of Gulf Stream water.

To compare shelf water flows with shifts in the Gulf Stream position, we traced the Gulf Stream frontal border on the images of Figure 4. This was done with the aid of near-surface ADCP velocity data acquired 10 h before and after the time of each image, which for all but one image encompasses the Gulf Stream front. Our representation of the border indicate that the point of Gulf Stream frontal separation from the continental margin shifted abruptly southward between survey phases 1 and 2, and migrated northward throughout the rest of the survey.

3.3. Moored Velocity and Temperature Observations

Data from the moored thermistors show the upper slope water column to be highly stratified throughout our study period (5–12 August), with a 12–24°C thermocline spanning a depth range of roughly 10–30 m (Figure 5). Throughout most of the study period, 8–12°C water with weak vertical temperature stratification (~0.1°C m^{-1}) appears beneath the thermocline. Based on the Scanfish T/S data acquired over the upper slope near the mooring, we identify this 8–12°C water as part of the cold pool. A warming event appears in the thermistor data on 11 August, with the 8–12°C subthermocline water displaced by 14–16°C water and with a 3°C increase in near-surface temperature (Figure 5). This event coincides with SST imagery showing an onshore intrusion of Gulf Stream water near the mooring (Figure 4) and is thus very likely due to the intrusion.

The along-slope (north-south) flow measured by the moored ADCP is predominantly unidirectional over the water column (Figure 5) and undergoes two reversals during the survey period: from northward-to-

southward during survey phase 2 and returning to northward during phase 3. Flow in both directions is relatively strong, with the southward (northward) velocity magnitude reaching 0.4 (0.3) m s^{-1}. At 8 days in length, the velocity record is too short for determining a meaningful statistical relationship between the currents and the near-surface wind. Nevertheless, the wind and ADCP-measured velocities appear to be related in a manner consistent with along-slope wind forcing of the along-slope current. Variations in the northward flow are similar to variations in the northward wind velocity, lagging the wind variations by $\sim$0.5 h. However, in view of the large variation in Gulf Stream frontal configuration and point of Gulf Stream separation from the continental margin (which shifts southward during the period of southward ADCP-measured flow and migrates northward when the flow is to the north), we cannot discount the possibility that the along-slope velocities measured by the ADCP are, in part, influenced by Gulf Stream frontal movements.

The east-west (across-slope) velocities often exhibit a complex vertical structure (Figure 5). At no levels are the east-west velocities clearly related, by visual inspection, to either the north-south or east-west (not shown) wind velocity.

Notably, during the appearance of warm water over 11–12 August, strong (order 0.25 m s^{-1}) westward (onshore) velocities are observed, an indication that this water is part of an intrusion of Gulf Stream water actively advected onto the shelf as suggested by the SST imagery of the period (Figure 4).

The depth and time-averaged east-west velocity is, with a mean of 0.0025 m s^{-1} and a 90% confidence interval of 0.02 m s^{-1}, essentially zero. Within a given ADCP measurement bin, mean east-west velocities are larger, with mean westward (onslope) velocities reaching 0.05 m s^{-1} in the upper 20 m and mean eastward (offslope) velocities reaching 0.024 m s^{-1} in the depth range of the cold pool water. However, none of these mean velocities are significantly different from zero within the 90% confidence interval.

3.4. Shelf Water Flow Patterns

A prominent feature seen throughout our survey is a well-defined jet of subpynocline cold pool water flowing southward along transect 1 (Figure 1). This is, very likely, a southern extension of the shelf-edge frontal jet [*Linder and Gawarkiewicz*, 1998; *Fratantoni et al*., 2001; *Gawarkiewicz et al*., 2008]. In data from all measurement phases with multiple across-shore transects (phases 1, 3, 4, and 5) evidence of this jet is absent along the southernmost transect (transect 3 in Figure 1). This pattern of cold pool water loss over our Scanfish survey area is illustrated here by the salinity and along-slope velocity fields of survey phase 3 (Figure 6). The southward cold pool water jet appears along the northern most transect (transect 1) where it reaches a maximum velocity in excess of 0.4 m s^{-1} and has a width of order 10 km. The cold pool water jet is seen transect 2, but with a sharply reduced width (order 4 km) and maximum current (0.3 m s^{-1}). Cold pool water is absent along transect 3.

As illustrated here by cold pool velocities at 35 m (Figure 7), details of the cold pool water flow vary significantly from one survey phase to the next. Of particular note are changes in the southward extent of the cold pool water jet. For example, the velocities from phases 1 and 2 indicate an abrupt southward shift in the jet's terminus. In phase 1, the jet is sharply attenuated between transects 1 and 2, going from a maximum speed of 0.33 to 0.11 m s^{-1}, and is absent from transect 3. In phase 2, the jet appears with significant strength at transect 2 (the only E-W transect of the phase), with southward velocities reaching 0.4 m s^{-1}. The terminus of the jet appears to migrate northward over phases 3–5. In phase 5, cold pool water flow is directed southward only at transect 1, with velocity of no greater than 0.12 m s^{-1}.

These latitudinal shifts in the termination of the cold pool water jet may be in part due to wind forcing. The jet shifts southward when the wind is to the south and migrates northward during a period of northward winds (Figure 7). However, the changing Gulf Stream position is strongly implicated as a mechanism influencing the jet's southward extent, as the latitude of the jet's terminus is closely linked with the point at which the Gulf Stream separates from the continental margin (Figure 7). In addition, the cold pool water velocities often vary significantly across a transect in a manner which suggest that the flow over the shelf and upper slope ($<$100 m depth) is more strongly influenced by wind forcing than the flow over deeper water. The 35 m deep cold pool velocities measured during phases 4 and 5, for example, are directed northward (in the wind direction) over depths $<$100 m, and southward over greater bottom depths (Figure 7).

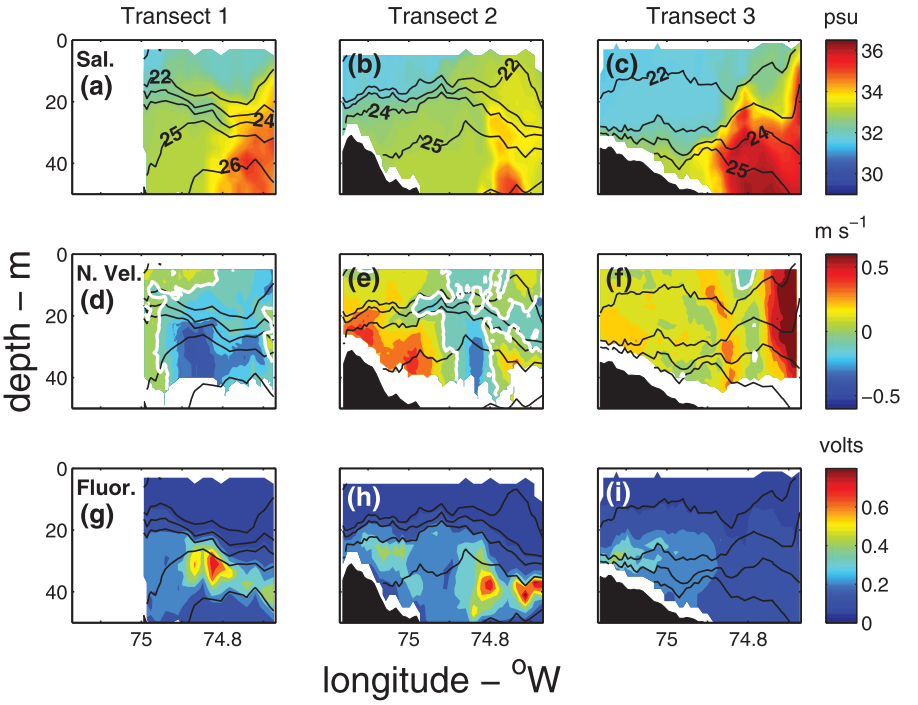

Figure 6. Fields of (a–c) salinity, (d–f) north-south velocity (positive to the north), and (g–i) fluorometer voltage (F_V) measured along transects (Figures 6a, 6d, and 6g) 1, (Figures 6b, 6e, and 6h) 2, and (Figures 6c, 6f, and 6i) 3 (Figure 1) during survey phase 3. Black lines in all plots are σ_T contours, and white lines on the velocity fields mark the zero-velocity contour.

The flow of near-surface shelf water also exhibits significant phase-to-phase variation over the 7 days of our survey (Figure 8). Mirroring the pattern of cold pool water flow, the latitudinal extent of the southward near-surface shelf water flow shifts southward between phases 1 and 2 and subsequently migrates northward. In addition, the changes of the near-surface shelf water flow appear to be related to variations in both the local wind and the Gulf Stream position.

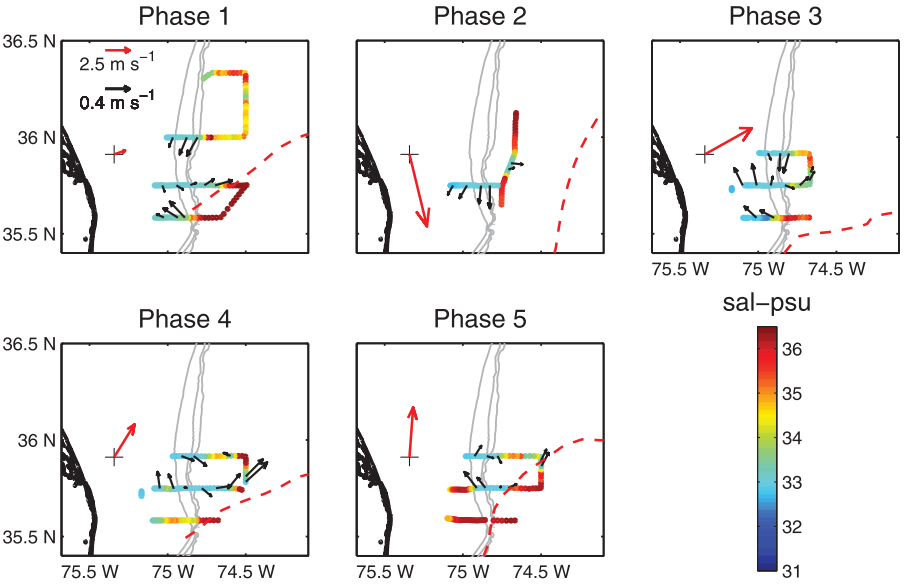

Figure 7. For the indicated phases, plots of salinity and cold pool water ($S < 34$ psu; $24 < \sigma_T < 26.4$) velocity at 35 m. Velocities of other water types are not displayed. Also shown are the mean wind velocity measured at buoy 44014 during each phase (red vector with origin displaced from the 44014 location to constrain the latitude bounds) and the northwestern edge of the Gulf Stream as determined from SST imagery (Figure 4). Gray lines mark the 60, 100, and 200 m isobaths.

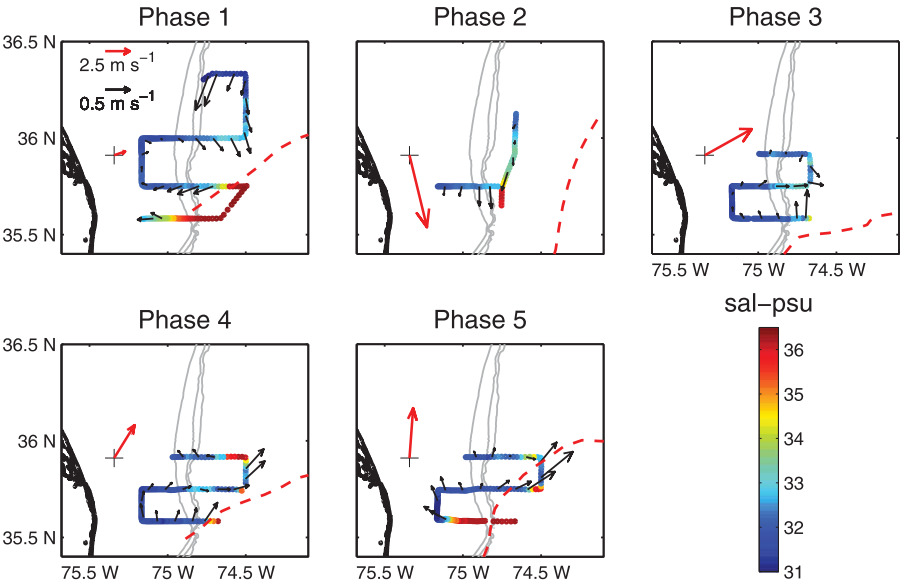

Figure 8. Same as Figure 7, except showing salinity and shelf water (S < 34 psu) velocity at 7 m.

Because high values of F_V within shelf water are largely confined to the cold pool, the transport of shelf water chlorophyll is principally tied with the flow of cold pool water. This is illustrated by the F_V and southward velocity fields of phase 3 (Figure 6). The fields along transect 1 show an area of high F_V situated within cold pool water immediately beneath the pycnocline. This encompasses a southward current of ~0.35 m s^{-1}. A similar band of southward moving cold pool water with high F_V is seen in the fields of transect 2, but with a much smaller horizontal extent than the band seen along transect 1.

The phase 3 fields along transect 3 reveal northward-moving near-bottom water with elevated F_V in the area where the pycnocline (shelf-edge front) intersects the bottom (Figure 6i). Similar features of northward-moving chlorophyll-enriched water appear in the area of the pycnocline-bottom intersection during phases 4 and 5. These features could be partly the result of enhanced sediment resuspension in the region of pycnocline-bottom intersection, due to the injection of biogenic bottom material (phaeopigments) into the water column and/or primary production stimulated by resuspended nutrients. High bottom stress and enhanced sediment resuspension due to the dissipation of internal wave energy in the bottom boundary layer have been observed in the area of the pycnocline-bottom intersection by a number of investigators [*Bogucki et al.*, 1997; *MacIntyre et al.*, 1999; *Klymak and Moum*, 2003; *Hosegood et al.*, 2004]. Another possible factor contributing to these features is upwelling in the area of the frontal intersection with the bottom, which may inject nutrients and/or resuspended biogenic material into the water column along frontal isopycnals. Upwelling at a frontal/bottom intersection has been indicated through theoretical calculations [*Gawarkiewicz and Chapman*, 1992; *Chapman and Lentz*, 1994] and observations [*Houghton*, 1997; *Barth et al.*, 1998; *Houghton and Visbeck*, 1998]. It is possible that enhanced resuspension and upwelling at the frontal/bottom intersection may have acted in concert to produce the patches of high F_V seen at the foot of the front during phases 3–5, with internal wave dissipation injecting bottom material into the water column and upwelling along frontal isopycnals carrying this material further upward and seaward.

An issue of interest is the extent to which chlorophyll carried into our study region along transect 1 is contained within the southward-flowing cold pool jet, i.e., is the jet a principal conduit for the transport of chlorophyll into the southern MAB? To address this issue, we determined the distribution of F_V in shelf water as a function of north-south velocity (v_N) across transect 1. This was done by first interpolating F_V, salinity and v_N onto a common grid, and then averaging shelf water F_V over 0.1 m s^{-1} v_N bands. For all but phase 5, the averages indicate a strong tendency for chlorophyll-rich water to be contained within the jet passing transect 1 (Figure 9). The F_V averages for phases 2 and 3, in particular, are more than four times higher in the −0.5 to −0.3 m s^{-1} v_N bands than in the bands of $v_N > -0.1$ m s^{-1} (southward v_N is negative). By contrast, the transect 1 F_V averages of phase 5 are not dominant in any v_N band, having nearly equal magnitudes over bands extending from −0.3 to 0.4 m s^{-1}. During phase 5, the Gulf Stream separation is at its

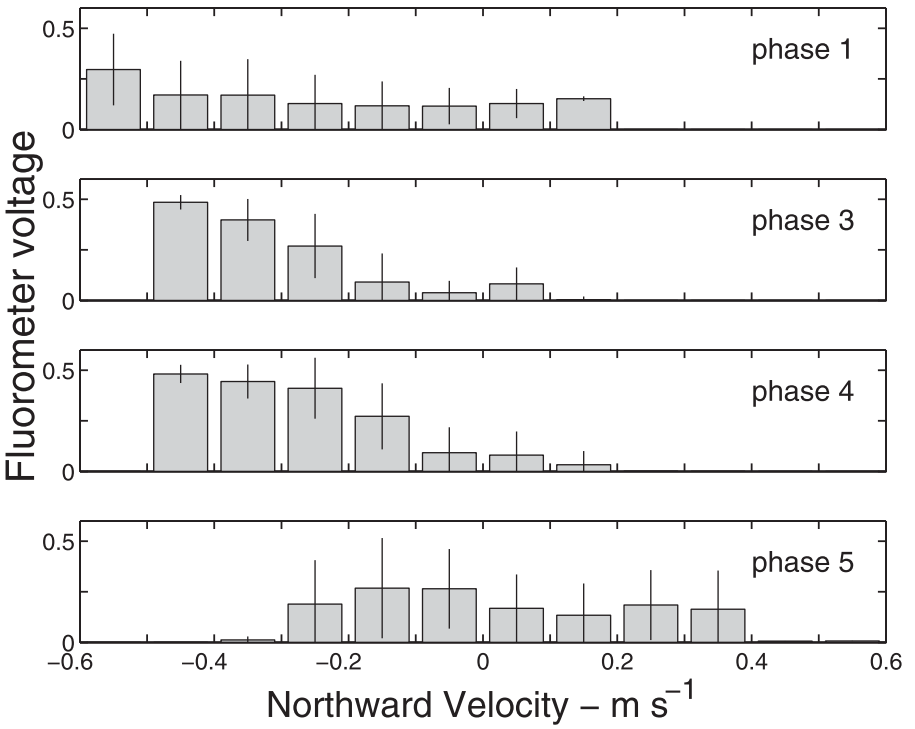

Figure 9. For each indicated phase, means of fluorometer voltage (F_V), and the standard deviation about each mean (vertical lines) of MAB shelf water (S < 34 psu) passing transect 1 (Figure 1). Each mean has been calculated over a 0.1 m s^{-1} band of north-south (positive to the north) velocity.

northernmost extent of our survey, abutting transect 1 (Figure 4), and the cold pool water jet appears to be near its southern terminus at transect 1 (Figure 7). We posit that the phase 5 measurements at transect 1 capture both the southward flow of chlorophyll-rich shelf water entering our study region and the northward flow of chlorophyll-rich shelf water exiting the region at the edge of the Gulf Stream.

3.5. Volume and Chlorophyll Transports of Shelf Water

Shelf water transport across each Scanfish section was determined from fields of salinity and velocity (perpendicular to the section) interpolated to a common grid. Transports were calculated for cold pool ($24 < \sigma_T < 26.4$) and lower-density ($\sigma_T < 24$; pycnocline/near-surface) shelf water masses, according to

$$T_i = \int\int^{A_i} v_\perp da$$

where T_i is the transport of water mass i (cold pool or lower-density shelf water), A_i is the cross-sectional area of the Scanfish section occupied by the water mass and $v_\perp$ is the velocity normal to the section. Also, calculated was the transport of fluorometer voltage (F_V transport) across each Scanfish section, a proxy for chlorophyll transport, according to

$$F_i = \int\int^{A_i} v_\perp F_V da$$

Transports were calculated for the portions of each section situated over the slope and rise seaward of the 100 m isobath. Because of the depth limitation of the ADCP data, the vertical band over which transports were computed was confined to 5–40 m. The computed transports thus represent a fraction of the overall shelf water transport through the southern MAB.

The volume transports (Figure 10 and Table 1) clearly show the latitudinal variations in the terminus of the southward shelf water flow over the slope and rise during our study, with the terminus shifting southward

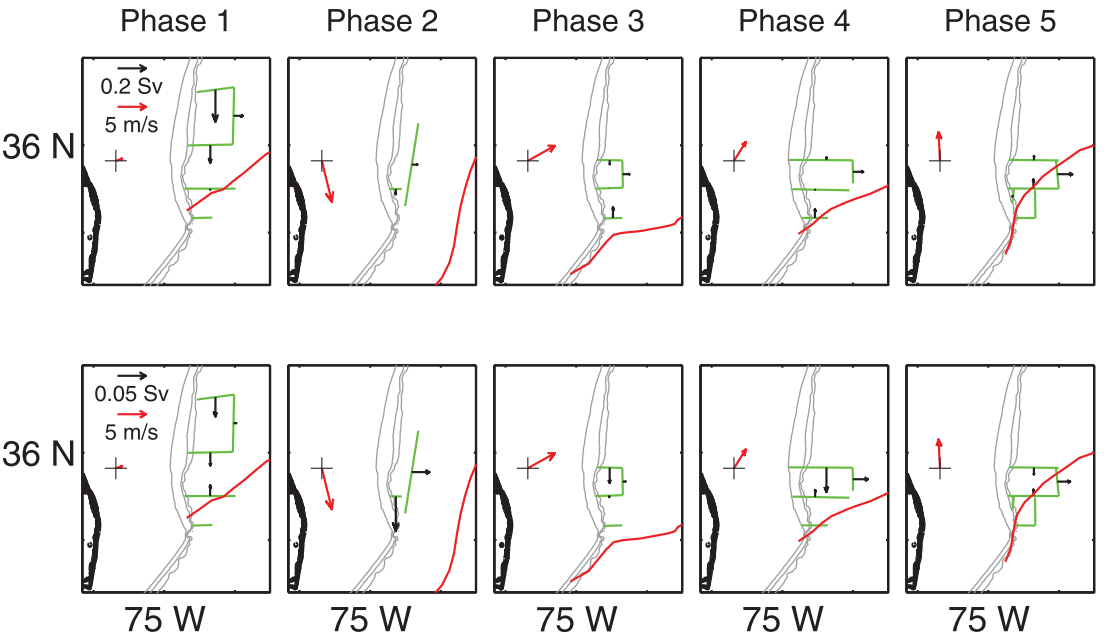

Figure 10. Estimated volume transport of MAB shelf water ($S < 34$ psu) across the indicated Scanfish lines and over the indicated survey phases. The bottom plots show the transport of cold pool water ($24 < \sigma_T < 26.4$), whereas the top plots show the transport of lower density ($\sigma_T < 24$; pycnocline and surface mixed layer) water (scales of the transports of the top and bottom plots differ). Also shown are the mean wind velocity measured at buoy 44014 during each phase (red vector with origin displaced from the 44014 location to constrain the latitude bounds) and the northwestern edge of the Gulf Stream as determined from SST imagery (Figure 4). Gray lines mark the 60, 100, and 200 m isobaths.

between phases 1 and 2 and migrating northward over phases 3–5. As the transports of cold pool water are determined from flows over depths >100 m and isolated from the surface by the seasonal pycnocline, these transports are not likely to be significantly influenced by the surface wind. The latitudinal shifts in the terminus of the cold pool transport are thus most likely due to changes in the position of the Gulf Stream's separation from the continental margin, which mirror the shifts in the cold pool flow termination (Figure 10).

While the volume transport of pycnocline/near-surface shelf water is often similar to the volume transport of cold pool water (Figure 10 and Table 1), it occasionally differs from cold pool transport in a manner consistent with a greater influence of surface wind forcing on the surface and pycnocline flow. Such a difference in cold pool versus upper water transport is particularly apparent over transect 1 in phases 4 and 5, during which the near-surface/pycnocline volume transport is directed northward, with the wind, and the cold pool transport is directed southward.

Pycnocline/near-surface volume transports typically (but not always) exceed cold pool volume transports. However the transport of F_V is typically more than four times greater in the cold pool than in the waters above (Figure 11 and Table 2), reflecting the propensity of cold pool water samples to have significantly higher F_V than the water above.

A notable feature seen in the volume and F_V transports of cold pool water over phases 3 and 4 is a relatively large southward transport over the northernmost east-west transect (transect 1) which is not balanced by the transports across downstream transects (to the south and east). This imbalance could be the result of subduction of cold pool water after passing transect 1, shifting part of the cold pool flow seen at transect 1 below the ADCP measurement range (of ~40 m). The Scanfish data offer marginal evidence that the cold pool water observed along transect 1 may subduct upon turning eastward toward the Gulf Stream. The nominal upper level of the cold pool, the $\sigma_T = 24$ surface, is 2–5 m deeper along the N-S transect between transects 1 and 2 than along transect 1.

4. Discussion

The basic features of the chlorophyll distribution determined from our August 2004 survey data are similar to those reported by *Wood et al.* [1996] based on measurements acquired over the MAB shelf

Table 1. Volume Transports (mSv, Positive to the North) of Cold Pool ($S < 34$ psu, $24 < \sigma_T < 26.4$; in Square Brackets) and Lower Density ($S < 34$ psu, $\sigma_T < 24$) MAB Shelf Water Across the East-West Transects of the Scanfish Surveys (Figure 1)[a]

Transect (Figure 1)	Phase 1 (5–6 Aug)	Phase 2 (7–8 Aug)	Phase 3 (9 Aug)	Phase 4 (9–10 Aug)	Phase 5 (10–11 Aug)
0	−227 [−34]				
1[b]	−127 [−23]		−29 [−27]	20 [−43]	29 [−12]
2	−11 [19]	−37 [−61]	3 [−3]	0 [12]	65 [11]
3	0 [0]		77 [0]	63 [0]	0 [0]

[a]Note that these values are shown to illustrate the north/south trend in the latitude at which the southward shelf water flow terminates. They should not be taken as the total shelf water transport over the slope and upper shelf as they are based on ADCP data from the 5 to 40 m depth band. In addition, the transect lengths differ from phase to phase (Figure 10).

[b]The latitude of transect 1 is 36°00′ for phase 1 and 35°55′ for phases 3–5.

and slope near Cape Hatteras in July 1993. In both data sets, high chlorophyll concentrations are principally contained within the cold pool and confined to the 24–26 σ_T range. Furthermore, the high chlorophyll concentrations observed in both data sets are largely at depths >20 m, beyond the order 10 m depth range over which pigments in MAB surface waters can be detected by satellite-based fluorometers [*Ryan et al*., 1999]. This contrasts with the analysis of *Ryan et al*. [1999], which shows an enhancement of chlorophyll concentrations at the MAB shelf edge, as detected by Coastal Zone Color Scanner imagery, during the mid-April to late-June transition from well-mixed to stratified conditions. *Ryan et al*. show a sample cross-shelf/slope section from early June in which high chlorophyll concentrations are contained within the 24–26 σ_T range, as observed in our observations and those of *Wood et al*. [1996], but extend to within a few meters of the surface (their Figure 4). The above observations raise the possibility of a seasonal variation in accessibility of chlorophyll-rich water near the MAB shelf-edge front to satellite-based fluorometry. As a cautionary note for interpreting the satellite-derived chlorophyll fields from the MAB shelf-edge region, it must be recognized that this region may often contain chlorophyll-rich water beneath the range of detection by satellite-based fluorometers.

Our measurements indicate, for the first time, that the chlorophyll-rich water contained within the cold pool is carried rapidly southward in the shelf-edge frontal jet at a rate of up to 0.6 m s^{-1}. The entrainment of this biogenic-rich transport into the Gulf Stream near Cape Hatteras likely has a substantial, but yet to be determined, impact on the carbon budget of coastal waters off of the northeast U.S.

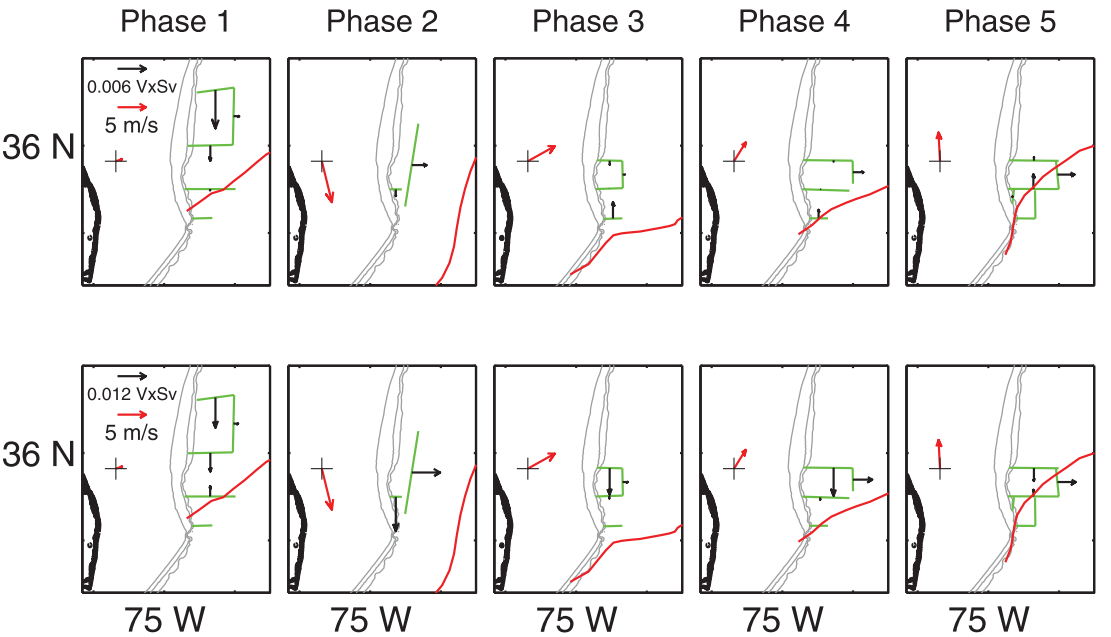

Figure 11. Same as Figure 10, except showing the cross-sectional integral of the product of fluorometer voltage (F_V) and across-transect velocity of (bottom) cold pool and (top) lower-density shelf water.

Table 2. Same as Table 1, Except Showing the Cross-Sectional Integral of the Product of Fluorometer Voltage (F_V) and Across-Transect Velocity (F_V Transport, V*mSv) for Cold Pool and Lower Density MAB Shelf Water

Transect (Figure 1)	Phase 1 (5–6 Aug)	Phase 2 (7–8 Aug)	Phase 3 (9 Aug)	Phase 4 (9–10 Aug)	Phase 5 (10–11 Aug)
0	−8.1 [−12.9]				
1	−3.2 [−7.9]		−0.9 [−11.3]	−0.3 [−11.9]	0.7 [−5.6]
2	−0.3 [4.2]	−1.5 [−14.6]	−0.04 [−1.0]	0.1 [−1.0]	3.1 [2.8]
3	0 [0]		3.5 [0]	1.8 [0]	0 [0]

Our analysis reveals a tight coupling between the location of the Gulf Stream's separation from the continental margin and the latitude at which the cold pool water is deflected offshore. The possibility that the movement of the Gulf Stream front may influence the upper-slope flow (at 80 m depth), with the flow following the Gulf Stream frontal movements (i.e., northward flow associated with northward frontal migration), is also indicated. This possible relationship between the frontal position and the upper-slope flow is consistent with analysis of satellite altimeter and SST data by *Bohm et al*. [2006], which revealed a southward acceleration (deceleration) of the flow associated with offshore (onshore) movement of the Gulf Stream front. However, as our mooring data set is only 8 days in duration, we cannot discern with statistical confidence the extent to which the observed flow variations are the product of Gulf Stream or wind forcing.

Of note are the rapid north-south shifts in the Gulf Stream frontal separation from the continental margin and the associated latitudinal shifts of cold pool water export. During the course of our study, the position of Gulf Stream separation varies by order 50 km, with the location of the cold pool water export undergoing a similar change. This coupled translation of the cold pool export zone and the Gulf Stream frontal separation likely has a significant impact on the movement and accumulation biogenic material over the Hatteras slope and rise. It is possible, for example, that areas within this translation band may alternately experience particle deposition, due to particle fallout during cold pool water passage, and erosion when exposed to the Gulf Stream. A result may be the net transfer of particles, via Gulf Stream transport, to depths beyond the continental slope. Such a possibility puts into question the estimates of the percent of MAB production sequestered in deep sediments, as most of these are based on analysis of core samples from the slope region, at depths <1200 m [*Alperin et al*., 2002; *DeMaster et al*., 2002; *Thomas et al*., 2002]. Developing a fuller understanding of the complex processes influencing the movement and ultimate fate of MAB shelf water and biogenic material exported from the Hatteras shelf and slope region clearly requires in-depth observational studies directed at these processes.

Acknowledgments
We are grateful to Captain James Warrington and the crew of the *R/V Cape Henlopen* for expert support of the scientific operations during the FINCH 2004 summer cruise. Our thanks go to B. Kidd and C. Marquette for their work in acquiring the data during the cruise. Particular thanks go to F. Bahr and C. Linder who participated in the cruise operations and contributed significantly to the analysis of the data presented here, and to I. Walsh who offered valuable advise with regard to analysis of the fluorometer data. This work was supported by the U.S. National Science Foundation through grants OCE-03–27249 and OCE-0926999.

References

Alperin, M. J., I. B. Suayah, L. K. Benninger, and C. S. Martens (2002), Modern organic carbon burial fluxes, recent sedimentation rates, and particle mixing rates from the upper continental slope near Cape Hatteras, North Carolina (USA), *Deep Sea Res., Part II*, *49*, 4645–4665.

Barnard, A. H., and T. O. Mitchell (2013), Biogeochemical monitoring of the oceans using autonomous profiling floats, *Ocean News Technol.*, *19*(2), 16–17.

Barth, J. A., D. Bogucki, S. D. Pierce, and P. M. Kosro (1998), Secondary circulation associated with a shelfbreak front, *Geophys. Res. Lett.*, *15*, 2761–2764.

Bigelow, H. B. (1933), Studies of waters on the continental shelf, Cape Cod to Chesapeake Bay. The cycle of temperature, *Pap. Phys. Oceanogr. Meteorol.*, *2*, 1–135.

Bignami, F., and T. S. Hopkins (2003), Salt and heat trends in the shelf waters of the southern Middle-Atlantic Bight, *Cont. Shelf Res.*, *23*, 647–667.

Blanton, B. O., R. A. Luettich, F. Werner, and H. Seim (2004), Barotropic tides in the South Atlantic Bight, *J. Geophys. Res.*, *109*, C12024, doi:10.1029/2004JC002455.

Bogucki, D., T. Dickey, and L. G. Redekopp (1997), Sediment resuspension and mixing by resonantly generated internal solitary waves, *J. Phys. Oceanogr.*, *27*, 1181–1196.

Bohm, E., T. S. Hopkins, L. J. Pietrafesa, and J. H. Churchill (2006), Continental margin slope sea level and flow variability induced by lateral movements of the Gulf Stream in the Middle Atlantic Bight, *Prog. Oceanogr.*, *70*, 196–212.

Chapman, D. C., and R. C. Beardsley (1989), On the origin of shelf water in the Middle Atlantic Bight, *J. Phys. Oceanogr.*, *19*, 384–391.

Chapman, D. C., and S. J. Lentz (1994), Trapping of a coastal density front by the bottom boundary layer, *J. Phys. Oceanogr.*, *24*, 1464–1479.

Churchill, J. H., and T. J. Berger (1998), Transport of Middle Atlantic Bight shelf water to the Gulf Stream, *J. Geophys. Res.*, *103*, 30,605–30,621.

Churchill, J. H., and P. C. Cornilion (1991a), Water discharged from the Gulf Stream north of Cape Hatteras, *J. Geophys. Res.*, *96*, 22,227–22,243.

Churchill, J. H., and P. C. Cornilion (1991b), Gulf Stream water on the shelf and upper slope north of Cape Hatteras, *Cont. Shelf Res.*, *11*, 409–431.

Churchill, J. H., and G. G. Gawarkiewicz (2012), Pathways of shelf water export from the Hatteras shelf and slope, *J. Geophys. Res.*, *117*, C08023, doi:10.1029/2012JC007995.

Churchill, J. H., P. C. Cornillon, and P. H. Hamilton (1989), Velocity and hydrographic structure of subsurface shelf water at the Gulf Stream's edge, *J. Geophys. Res.*, *94*, 10,791–10,800.
DeMaster, D. J., R. H. Pope, L. A. Levin, and N. E. Blair (1994), Biological mixing intensity and rates of organic carbon accumulation in North Carolina slope sediments, *Deep Sea Res., Part II*, *41*, 735–753.
DeMaster, D. J., C. J. Thomas, N. E. Blair, W. L. Fornes, G. Plaia, and L. A. Levin (2002), Deposition of bomb 14C in continental slope sediments of the Mid-Atlantic Bight: Assessing organic matter sources and burial rates, *Deep Sea Res., Part II*, *49*, 4667–4685.
Fisher, A. (1972), Entrainment of shelf water by the Gulf Stream northeast of Cape Hatteras, *J. Geophys. Res.*, *77*, 3248–3255.
Flagg, C. N., D. Wallace, and Z. Kolber (1998), Cold anticyclonic eddies formed from cold pool water in the southern Middle Atlantic Bight, *Cont. Shelf Res.*, *17*, 1839–1867.
Ford, W. L., J. R. Longard, and R. E. Banks (1952), On the nature, occurrence and origin of cold low salinity water along the edge of the Gulf Stream, *J. Mar. Res.*, *11*, 281–293.
Fratantoni, P. S., R. S. Pickart, D. J. Torres, and A. Scotti (2001), Mean structure and dynamics of the shelfbreak jet in the Middle Atlantic Bight during fall and winter, *J. Phys. Oceanogr.*, *31*, 2135–2156.
Gawarkiewicz, G., and D. C. Chapman (1992), The role of stratification in the formation and maintenance of shelfbreak fronts, *J. Phys. Oceanogr.*, *22*, 753–772.
Gawarkiewicz, G., J. Churchill, F. Bahr, C. Linder, and C. Marquette (2008), Shelfbreak frontal processes north of Cape Hatteras in winter, *J. Mar. Res.*, *66*, 775–799.
Gawarkiewicz, G. G., and C. Linder (2006), Lagrangian flow patterns north of Cape Hatteras using near-surface drifters, *Prog. Oceanogr.*, *70*, 181–195.
Han, G., and T. Niedrauer (1981), Hydrographic observations and mixing processes in the New York Bight, 1975–1977, *Limnol. Oceanogr.*, *26*, 1126–1141.
Hosegood, P., J. Bonnin, and H. van Haren (2004), Solibore-induced sediment resuspension in the Faeroe-Shetland Channel, *Geophys. Res. Lett.*, *31*, L09301, doi:10.1029/2004GL019544.
Houghton, R. W. (1997), Lagrangian flow at the foot of a shelfbreak front using a dye tracer injected into the bottom boundary layer, *Geophys. Res. Lett.*, *24*, 2035–2038.
Houghton, R. W., and M. Visbeck (1998), Upwelling and convergence in the Middle Atlantic Bight shelfbreak front, *Geophys. Res. Lett.*, *25*, 2765–2768.
Houghton, R. W., R. Schlitz, R. C. Beardsley, B. Butman, and J. L. Chamberlin (1982), Middle Atlantic cold pool: Evolution of the temperature structure during summer 1979, *J. Phys. Oceanogr.*, *12*, 1019–1029.
Klymak, J. M., and J. M. Moum (2003), Internal solitary waves of elevation advancing on a shoaling shelf, *Geophys. Res. Lett.*, *30*(20), 2045, doi:10.1029/2003GL017706.
Kupferman, S. L., and N. Garfield (1977), Transport of low-salinity water at the slope water-Gulf Stream boundary, *J. Geophys. Res.*, *82*, 3481–3486.
Lillibridge, J. L., III, G. Hitchcock, T. Rossby, E. Lessard, M. Mork, and L. Golmen (1990), Entrainment and mixing of shelf/slope waters in the near surface Gulf Stream, *J. Geophys. Res.*, *95*, 13,065–13,087.
Linder, C. A., and G. G. Gawarkiewicz (1998), A climatology of the shelfbreak front in the Middle Atlantic Bight, *J. Geophys. Res.*, *103*, 18,405–18,423.
Lohrenz, S., D. G. Redalje, P. Verity, and C. Flagg (2002), Primary production on the continental shelf off Cape Hatteras, North Carolina, *Deep Sea Res., Part II*, *49*(20), 4479–4509.
Luettich, R. A., J. J. Westerink, and N. W. Scheffner (1992), ADCIRC: An advanced three-dimensional circulation model for shelves, coasts and estuaries, Report 1: Theory and methodology of ADCIRC-2DDI and ADCIRC-3DL, *Tech. Rep. DRP-92-6*, U.S. Army Eng., Waterways Exp. Stn., Vicksburg, Miss.
MacIntyre, S., K. M. Flynn, R. Jellison, and J. R. Romero (1999), Boundary mixing and nutrient fluxes in Mono Lake, California, *Limnol. Oceanogr.*, *44*, 512–529.
Proctor, C. W., and C. S. Roesler (2010), New insights on obtaining phytoplankton concentration and composition from in situ multispectral chlorophyll fluorescence, *Limnol. Oceanogr. Methods*, *8*, 695–708.
Ryan, J. P., J. A. Yoder, and P. C. Cornillon (1999), Enhanced chlorophyll at the shelfbreak of the Mid-Atlantic Bight and Georges Bank during the spring transition, *Limnol. Oceanogr.*, *44*, 1–11.
Savidge, D. K., and J. A. Austin (2007), The Hatteras Front: August 2004 velocity and density structure, *J. Geophys. Res.*, *112*, C07006, doi: 10.1029/2006JC003933.
Savidge, D. K., J. A. Austin, and B. O. Blanton (2013a), Variation in the Hatteras Front density and velocity structure Part 1: High resolution transects from three seasons in 2004–2005, *Cont. Shelf Res.*, *54*, 93–105, doi:10.1016/j.csr.2012.11.005.
Savidge, D. K., J. A. Austin, and B. O. Blanton (2013b), Variation in the Hatteras Front density and velocity structure Part 2: Historical setting, *Cont. Shelf Res.*, *54*, 106–116, doi:10.1016/j.csr.2012.11.006.
Thomas, C. J., N. E. Blair, M. J. Alperin, D. J. DeMaster, R. A. Jahnke, C. S. Martens, and L. Mayer (2002), Organic carbon deposition on the North Carolina continental slope off Cape Hatteras (USA), *Deep Sea Res., Part II*, *49*, 4687–4709.
Verity, P. G., J. Bauer, C. N. Flagg, D. DeMaster, and D. Repeta (2002), The ocean margins program: An interdisciplinary study of carbon sources, transformations, and sinks in a temperate continental margin system, *Deep Sea Res., Part II*, *49*, 4273–4295.
Vodacek, A., N. V. Blough, M. D. DeGrandpre, E. T. Peltzer, and R. K. Nelson (1997), Seasonal variation of CDOM and DOC in the Middle Atlantic Bight: Terrestrial inputs and photooxidation, *Limnol. Oceanogr.*, *42*, 674–686.
Wood, A. M., N. D. Sherry, and A. Huyer (1996), Mixing of chlorophyll from the Middle Atlantic Bight cold pool into the Gulf Stream at Cape Hatteras in July 1993, *J. Geophys. Res.*, *101*, 20,579–20,593.